Polymer 146 (2018) 321–330

Contents lists available at ScienceDirect

Polymer

journal homepage: www.elsevier.com/locate/polymer

Internal antiplasticisation in highly crosslinked amine cured multifunctional epoxy resins

Roderick Ramsdale-Capper, Joel P. Foreman*

Department of Materials Science and Engineering, Sir Robert Hadfield Building, University of Sheffield, Sheffield, S1 3JD, UK

ARTICLE INFO

Article history:
Received 14 February 2018
Received in revised form
14 May 2018
Accepted 17 May 2018
Available online 18 May 2018

Keywords:
Internal antiplasticisation
TGAP
DDS
Epoxy
Thermoset
Crosslinking
Phenylene rings
Substitution effects

ABSTRACT

The aromatic epoxy isomers triglycidyl *p*-aminophenol and triglycidyl *m*-aminophenol were cured with two aromatic diamine isomers 4,4′ diaminodiphenyl sulphone and 3,3′ diaminodiphenyl sulphone, creating four variations of epoxy resin. Dynamic and static mechanical analyses were used to understand the influence of chemical and network structure on the thermal, volumetric and mechanical properties of the epoxy resin. Fracture toughness increases are observed for networks containing meta substituted phenylene ring amines compared to the para equivalents, however no difference is noticed when the meta substituted phenylene ring epoxy is used. Use of meta substituted phenylene rings increases glassy modulus, yield stress, density and strain to failure. Correspondingly, decreases are seen in the glass transition temperature, intensity of the beta transition and the rubbery modulus. The results are entirely consistent with internal antiplasticisation caused by the presence of the meta substituted phenylene rings.

1. Introduction

Aromatic, multi-functional epoxy resins cured with diamine hardeners are being extensively used as matrices within composite materials for structural aerospace applications [1]. This is due to their high stiffness and strength, as well as their good thermal properties, low shrinkage on cure and chemical resistance relative to other polymers [2]. Their high stiffness and strength is the result of the stiff aromatic backbone of both the epoxy resin and hardener molecules. Triglycidyl aminophenol (TGAP) has a nominal functionality >2, allowing for a greater degree of branching and crosslinking within the network structure. The diamine hardeners also have a functionality >2 as each amine group can react twice. However, the high degree of crosslinking causes brittleness in these epoxy resins due to a restriction in the mobility of the network structure.

The toughness of epoxy resins can be improved by altering the network structure or by adding fillers into the network. Network changes include improving the flexibility of the polymer chain, reducing the functionality of the epoxy resins or even reducing the degree of cure. The latter can be achieved either by changing the cure schedule or the ratio of epoxy to amine hydrogen groups. Network changes often show minor differences in the fracture toughness compared with the addition of rubber or thermoplastics [3–5]. Adding rubber or thermoplastic fillers to increase the toughness often compromises the stiffness and strength, as well as displaying a phase separated glass transition temperature and possibly initiating degradation sites. More recently, hyperbranched polymers (HBP) have been cured within the epoxy resin structure and have been shown to toughen the epoxy network structure [6–9]. However, in some cases a reduction in the glass transition temperature has been noted and also increased water absorption caused by polar groups which will affect the long-term properties of the material in service [9]. Some HBP resins may also have cost implications and complicated processing limiting the production scales [6]. For this reason, continued research is being done to fully understand the epoxy resin structure [10,11].

Adding toughening fillers such as rubber or thermoplastics plasticises the network structure of thermosets. Traditionally, plasticisation causes an increase in the fracture toughness (and often the size of the sub-ambient beta transition) whilst simultaneously decreasing the stiffness, strength, and glass transition temperature of the network. Conversely, certain fillers when added

* Corresponding author.
E-mail address: j.foreman@sheffield.ac.uk (J.P. Foreman).

https://doi.org/10.1016/j.polymer.2018.05.048

to a polymer result in the phenomenon of 'antiplasticisation'. The addition of an antiplasticising filler typically results in an increase in the stiffness and strength, whilst simultaneously increasing tear strength, fracture energy or impact strength [12–14]. The congruent increase in stiffness, strength and also fracture toughness as a result of antiplasticisation is a relatively counterintuitive concept since stiffness/strength is more traditionally inversely linked to toughness. However, adding antiplasticising additives does not always increase the fracture toughness, and the effect has been shown to be strain rate dependent [12].

Alongside improvements in stiffness, strength and fracture toughness, antiplasticisation also results in an increased density and reductions in the glass transition temperature, the intensity of the beta transition, the rubbery modulus and the strain to failure [15]. Fillers which cause an antiplasticising effect are often stiff polar molecules [12–14,16], for example pentachlorobiphenyl [13]. Such molecules exist within (and hence reduce) the unoccupied volume in the network. This results in a greater chance for intermolecular interactions to occur [16] and an increase in density of the network [12,17]. Reducing the unoccupied volume and increasing the cohesive energy causes observed increases in stiffness and strength. The high temperature region of the beta transition is commonly suppressed by antiplasticising additives [13,16–18]. This may be due to both the reduction in unoccupied volume and increased cohesive energy restricting more cooperative motions from occurring. The T_g is reduced due to a decreased crosslink density which increases the mobility of the network at elevated temperatures. Finally, the strain to failure decreases [12,14,19] because the filler acts to decrease plastic flow by filling unoccupied volume restricting the network.

The antiplasticisation phenomenon may also be caused by internal changes within the network, termed 'internal antiplasticisation'. These internal changes can be introduced by curing with different isomers, extending the polymer chains [20] or changing the epoxy resin to hardener ratio [21,22]. Internal antiplasticisation causes reduced unoccupied volume and increased cohesive energy which produces similar property changes to those observed by antiplasticising fillers. Namely, an increase in glassy modulus, yield strength and density and a reduction in glass transition temperature, the intensity of the beta transition and the rubbery modulus. However, the strain to failure is observed to *increase* with increasing internal antiplasticisation [11,23], contrary to the effect seen for antiplasticising fillers. The fracture toughness is observed to increase with increasing internal antiplasticisation [23] though no strain rate dependence was reported in this case.

Previously, resins consisting of the structurally isomeric diamines 4,4′diaminodiphenyl sulphone (44DDS) and 3,3′diaminodiphenyl sulphone (33DDS) cured with diglycidyl ether of bisphenol A (DGEBA) have been investigated [10,23]. These studies concluded that the meta substituted 33DDS causes internal antiplasticisation of the network, due to the restriction of the phenylene ring motion and conformational differences causing a reduction in unoccupied volume and an increase in cohesive energy. The stiffness, strength and density were reported to increase while the beta transition is supressed in the meta substituted 33DDS cured resin compared with the para substituted 44DDS equivalent.

The sub-T_g beta transition has previously been attributed to local cooperative motions within the epoxy resin network structure. Solid state NMR studies of deuterated DGEBA/DDS and DGEBA/4,4′methylene dianiline concluded that the beta transition in these epoxy resins is caused by three distinct motions [10,24]. Firstly, the lower temperature region of the beta transition is attributed to the phenylene ring motions within the epoxy parts of the network. Secondly, the middle region is attributed to the crankshaft motion of the hydroxypropyl ether parts of the network (the reacted epoxy groups). Thirdly, the higher temperature region is attributed to the phenylene ring motion of the diamine parts of the network. The chemical structures of the epoxies DGEBA and TGAP are similar enough that the conclusions from previous solid state NMR work on DGEBA/DDS can be applied here. The network structures of both resins contain phenylene rings and hydroxypropyl ether groups so the transitions can be compared with relative confidence. However, two structural differences between DGEBA and TGAP should be noted.

Firstly, DGEBA has two phenylene rings separated by a central $C(Me)_2$ group whereas TGAP has a single phenylene ring. The cooperative motion of two phenylene rings in either the epoxy or amine parts of the network has been shown to contribute to the size and shape of the beta transition [10]. With only a single phenylene ring in the epoxy part of a TGAP based network, such cooperative motion is not available, so the lower temperature region of the beta transition should be reduced in comparison to that in the equivalent DGEBA network. However, these effects may be masked by the higher temperature region of the beta transition which is caused by the diamine part of the network, and DDS is common to both TGAP and DGEBA based resins in this comparison.

Secondly, one half of the chemical structure of TGAP is similar to DGEBA with an ether group connecting the central phenylene ring to an epoxy. However, the other half of TGAP has an amine group connecting the central phenylene ring to the two other epoxy groups. This distinction may reduce the rotational freedom of the TGAP group compared to DGEBA. It is also therefore technically correct to refer to the presence of both hydroxypropyl ether *and* hydroxypropyl amine groups in cured TGAP resins. The crankshaft style motions of either are presumably responsible for the middle region of the beta transition referred to earlier.

Complicating matters further, another sub-T_g transition is often present in the temperature regions between the beta and glass transitions but the molecular origin of this effect is still a source of relative uncertainty. Nomenclature for this transition varies from author to author with no general consensus, so we have adopted the term 'omega transition'. It has previously been attributed to both the phenylene ring motions in the epoxy resin portion and hydrogen bonded hydroxypropyl ether groups [25,26]. Some authors relate it to the local motions present in low crosslinked regions [27–29], however it has also been mentioned that it is due to local motions within high crosslinked regions of the network [30]. More recently Tu and co-workers have suggested that it is a cooperative motion of the entire DGEBA segment within the cured network [10]. The latter argument has the advantage of being backed by the underlying physics of motion within the polymer network. The low temperature beta transition is caused by motions of physically smaller parts of the network (subsections of DGEBA or DDS), the omega transition would then be caused by motions of larger parts of the network (the entire DGEBA segments) and finally the glass transition is caused by motion of the entire network.

The properties of resins cured using a stoichiometric ratio of structural isomers of both TGAP and DDS have previously been reported [31]. It was shown that the para-para substituted TGAP/DDS network displayed a broader beta transition than any of the meta substituted equivalents. The three resins containing a meta substituted isomer (in either epoxy or amine) displayed a similar loss tangent ($\tan\delta$) curve over the beta transition range. This was related to the increased chance of cooperative motions available due to unreacted segments within para-para substituted TGAP/DDS. The reason for no variation in the meta substituted equivalents may be due to homo polymerisation which is known to occur

within the network during cure [1,32]. This would result in dangling ends within the structure in a stoichiometric sample which will cause the network to be plasticised. The stress strain curves of the different TGAP/DDS isomers were also measured and it was concluded that post yield strain softening was dependent on glass transition type motions. These include restricted rotation of the aminophenol segment in meta substituted TGAP or the conformational freedom in the meta substituted DDS segment. The latter has also been reported as the cause of strain softening in DGEBA cured with the para and meta substituted isomers of DDS [33].

The aim of this study is to investigate the impact of structural isomerism of both the epoxy and amine on the network structure of the cured resins. The internal antiplasticisation effect caused by switching from either the para epoxy or amine to the meta equivalents will be assessed. To our knowledge the significance of the isomeric changes in multi-functional epoxy resins and the link to internal antiplasticisation of the network structure has not been reported for the isomers of TGAP. Further, the link between internal antiplasticisation and the nature of the sub-T_g transitions in TGAP/DDS networks has not yet been reported in the literature. By understanding the effect of internal antiplasticisation in such resins, the use of traditional toughening approaches can be more accurately tailored.

2. Experimental

2.1. Materials

The epoxy resin isomers used are triglycidyl *p*-aminophenol (TGPAP) and triglycidyl *m*-aminophenol (TGMAP) (supplied as Araldite MY0510 and Araldite MY0610 respectively by Huntsman Advanced Materials). The amine isomers used are 4,4′diaminodiphenylsulphone (44DDS) (supplied by Sigma Aldrich) and 3,3′diaminodiphenylsulphone (33DDS) (supplied as Aradur 9719-1 by Huntsman Advanced Materials). The chemical structures of these molecules are shown in Fig. 1. When cured, four different epoxy resin sample types are created, denoted as TGPAP/44DDS, TGPAP/33DDS, TGMAP/44DDS and TGMAP/33DDS. The four sample types represent para-para, para-meta, meta-para and meta-meta combinations of the phenylene ring structural isomers respectively.

The three main reactions which occur during amine cure of the epoxy are illustrated in Fig. 2. The first is the reaction of an epoxy with a primary amine to create a secondary amine. This secondary amine will also react with an epoxy to create a tertiary amine. Finally, a reacted epoxy and an unreacted epoxy can react to create

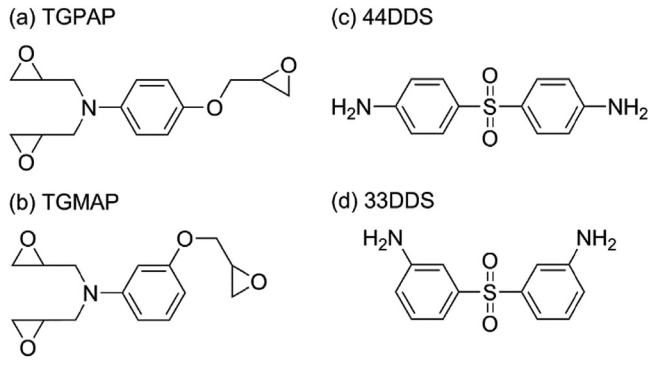

Fig. 1. Chemical structure of the monomeric epoxies and amines used (a) Triglycidyl *p*-aminophenol (TGPAP), (b) Triglycidyl *m*-aminophenol (TGMAP), (c) 4,4′diaminodiphenylsulphone (44DDS) and (d) 3,3′diaminodiphenylsulphone (33DDS).

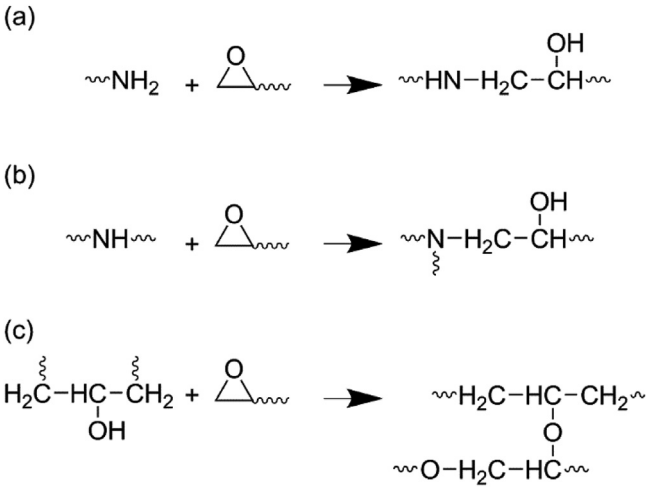

Fig. 2. Chemical reactions between epoxy and amine monomers to create a cured epoxy resin. (a) Primary amine reaction, (b) Secondary amine reaction and (c) Etherification.

an ether bridge; this final reaction is more likely in TGAP based resins cured at high temperatures [34,35]. The final cured resin is a highly crosslinked, thermoset 3D network polymer structure.

2.2. Preparation of epoxy resins

The stoichiometric ratio for pure TGAP cured with DDS based on their molecular weights and functionalities is 100:67. For this study an epoxy rich ratio of 100:36 is used. This is to account for differences in the theoretical and actual functionalities of the components, the difference in the epoxy equivalent weights of pure TGAP and MY0510/MY0610 as well as homopolymerisation during network cure. An epoxy excess is used in industry for TGAP-based resins to ensure the maximum amine conversion and also to reduce water ingress caused by unreacted amine groups. The uncured TGAP is initially heated to 60 °C to reduce its viscosity, after which the DDS is added. The temperature of the mixture is increased to 120 °C and mechanically stirred for approximately 30 min until the DDS has dissolved producing a clear homogeneous solution. The solution is then placed into a vacuum oven at 100 °C to degas and then poured into a preheated mould prior to cure.

Several different types of moulds were used to create different shaped cured resin, minimising the need for post processing and machining. Thin samples suitable for dynamic mechanical analysis (DMTA) used a flat sheet of toughened glass onto which the resin was carefully poured. Cylinders suitable for compression testing were made using small, thin glass test tubes. Thicker plaques of resin suitable for cutting into Single Edge Notched Beam (SENB) samples were made using a silicone mould. All mould surfaces were prepared using Frekote 770-NC release agent to aid demoulding after cure.

The cure cycle for curing on the glass sheet was 100 °C preheat temperature for the mould, ramp to 130 °C at 2 °C.min^{-1}, dwell at 130 °C for 1 h, ramp to 200 °C at 2 °C.min^{-1}, dwell at 200 °C for 2 h and finally ramp to 25 °C at 2 °C.min^{-1}. The cure cycle for the glass test tubes and the silicone mould was amended to avoid exothermic reactions. For the glass test tubes, ramp to 130 °C at 2 °C.min^{-1}, dwell at 130 °C for 2 h, ramp to 200 °C at 1 °C.min^{-1} and a dwell at 200 °C for 1.5 h. For the silicone mould, ramp to 130 °C at 2 °C.min^{-1}, dwell at 130 °C for 2 h, ramp to 160 °C at 2 °C.min^{-1}, dwell at 160 °C for 1 h, ramp to 200 °C at 1 °C.min^{-1} and dwell at 200 °C for 2 h. The differences in the cure between different moulds

were deemed negligible as the T_g's of the samples from each of these cures were within a 2 °C of each other. The samples were ground top and bottom to remove a thin layer to prevent issues with surface oxidation or remnants of the release agent affecting the resin properties. Samples were stored over phosphorous pentoxide to prevent moisture absorption.

2.3. Characterisation of materials

2.3.1. Differential scanning calorimetry (DSC)

A Perkin Elmer DSC6 was used to measure the heat flow as temperature is increased from which the degree of conversion of the epoxy resin can be calculated. For each test, a dynamic heating scan was used, increasing temperature from 30 °C to 290 °C at 10 °C.min^{-1}, then returning to room temperature at the same rate. This was repeated a second time to confirm full cure by measuring any residual exothermic heat flow or change in the T_g of the material. The samples were placed in closed aluminium pans with 5–8 mg of resin. At least 2 samples of each sample type were run.

A reference sample is completely cured in the DSC to simulate 100% cure and provide a reference value of the total enthalpy of cure, ΔH_{ref}. Following this, each of the oven cured samples is subjected to the same heating profile and the total residual enthalpy is measured, ΔH_{oven}. Finally, the degree of conversion can be calculated for each sample type using equation (1).

$$\alpha = \left(1 - \left(\frac{\Delta H_{oven}}{\Delta H_{ref}}\right)\right) \times 100 \quad (1)$$

2.3.2. Gas pycnometry

A Micromeritics AccupycII 1340 helium gas pycnometer was used to measure the volume of all samples by measuring the amount of gas displaced at 19.00 psi. Testing consisted of 25 cycles on three 10 mm diameter samples of each type at 27 °C. The density is then calculated after measuring the mass on a four point balance.

2.3.3. Dynamic mechanical thermal analysis (DMTA)

Samples cast onto the glass sheet were cut into rectangular coupons measuring 30 mm × 10 mm x 1.6 mm. A Perkin Elmer DMA8000 was used in single cantilever mode to measure the dynamic response in each sample as a result of applying a sinusoidal force at 1 Hz. The samples were scanned from −160 °C to 300 °C at a heating rate of 3 °C.min^{-1} using a strain amplitude of 0.05 mm. Six samples of each resin variant were tested to provide a statistically valid representation of the transitions occurring, particularly where they are broad and relatively low intensity (beta and omega transitions). The storage modulus, loss modulus and tanδ were recorded allowing for the tanδ peak transition temperature and the area under each peak to be calculated. Calculation of the peak areas was determined using OriginPro 8 software but this approach proved inconsistent. The calculated peak areas for the beta and omega transitions are particularly prone to noise and interference from neighbouring transitions or are outside machine temperature limits. As such, the peak area calculation data for the beta and omega transitions should be treated more as a qualitative indication of behaviour than a quantitative measurement.

2.3.4. Crosslink density

The crosslink density, ν_e, is determined using standard rubber elasticity theory which assumes that above the glass transition van der Waal's and other interactions between the molecules have been broken and what remains is proportional to the amount of crosslinking present in the network. This can be measured using the rubbery modulus, however in this work the rubbery storage modulus $E_{'}^{Rubbery}$ from the DMTA tests is used instead. This is not as accurate as using the static rubbery modulus, but any trends in the crosslink densities will be discernible. The crosslink density is calculated using equation (2) at $T = T_g + 30$ to ensure the network is in the rubbery phase. R is the universal gas constant.

$$\nu_e = \frac{E'_{Rubbery}}{3RT} \quad (2)$$

2.3.5. Static compression testing

Compression samples were cured in glass test tubes to produce cylindrical samples of 10 mm diameter which are then machined to 10 mm lengths with parallel faces. An Instron 5582 tensometer was used to measure the static compressive load-response properties of the samples. Five samples of each resin variant were tested at a strain rate of 1 mm min^{-1} at 30 °C. Strain was measured using standard cross-head separation distances and consequently a compliance correction was applied to the data to correct for strain anomalies. Yield stress and strain were defined as the stress/strain at which the sample first displays a zero gradient stress-strain curve.

2.3.6. Single Edge Notched Beam testing (SENB)

SENB samples were machined from larger plaques cured in the silicone mould to dimensions 50 mm × 10 mm x 4 mm. A pre-crack of variable length was created in each sample by tapping a fresh razor blade directly into the sample edge with a hammer. The pre-cracked samples were tested in three point bend mode (span 40 mm) using a Lloyd Instruments TA500 tensometer at 10 mm min^{-1} until the sample failed with a single crack into two clean halves. Compliance correction was also applied to the SENB data to correct for strain discontinuities. Testing was undertaken at 22 °C and the critical stress intensity factor and critical energy release rate are calculated to determine the fracture toughness of the materials. At least seventeen samples were tested for each sample type to ensure statistical validity.

3. Results and discussion

3.1. Differential scanning calorimetry

The results for the degree of conversion (α) analysis are given in Table 1. This shows α for the four sample types is greater than 98% so unreacted segments can be said to have minimal influence on the properties of the networks. In addition to this, α values for all four sample types are within 2% of one another and can therefore be considered to be similarly cured. This is a useful result because the value of α is directly related to the proportion of hydroxypropyl ether/amine groups present in the resin. Each reacted epoxy group creates a hydroxypropyl ether/amine group which contributes to the beta transition via a crankshaft style motion. If the degrees of conversion in the four sample types are all approximately the same, it follows that the proportion of hydroxypropyl ether/amine groups are the same. Consequently, this suggests that the hydroxypropyl ether/amine group contribution to the beta transition is equal in all four sample types. So, any differences observed in the beta transitions are therefore likely due to the other contributions, namely the rotation of the phenylene rings.

While the DSC results are useful for the analyses which follow, it must be acknowledged it is a relatively limited technique for measuring α. Complications may arise from its inability to

Table 1
Calculated degree of conversion, density, glass transition, omega transition and beta transition temperatures and the calculated beta transition area for the four sample types. The error expressed in the table is the standard deviation of the sample range.

Sample type	α/%	Density/g.cm^{-3}	T_g/°C	T_ω/°C	T_β/°C	Area of beta transition
TGPAP/44DDS	99.0 ± 0.1	1.3115 ± 0.0018	270 ± 1	64 ± 2	−37 ± 2	3.43 ± 0.26
TGPAP/33DDS	98.3 ± 0.5	1.3140 ± 0.0017	231 ± 1	91 ± 3	−43 ± 2	3.08 ± 0.33
TGMAP/44DDS	99.6 ± 0.1	1.3245 ± 0.0014	237 ± 1	–	−39 ± 1	2.86 ± 0.16
TGMAP/33DDS	99.8 ± 0.1	1.3254 ± 0.0014	212 ± 1	–	−43 ± 1	2.32 ± 0.22

distinguish between the different reactions illustrated in Fig. 2.

The differences between the curing kinetics of the four sample types can be observed from the DSC curves for the resin cure. Fig. 3 shows that the onset of the exothermic peak and therefore the initiation of cure occurs at a lower temperature for TGAP cured with meta substituted DDS compared to the para equivalents. This is a direct consequence of the increased nucleophilicity of the substituents in the meta isomers leading to a lower activation energy as fewer transition states exist. The corresponding para substituted phenylene ring therefore reacts at a higher temperature [36]. Fig. 3 also shows that meta substituted TGAP initiates at lower temperatures compared to the para equivalent for the same reason as in the DDS.

The lower cure initiation temperature for the meta substituted epoxy or amine has a noteworthy consequence on the resultant cured network structure. In the early part of the cure schedule, the temperature is lower and a dwell at 130 °C is maintained for some time. In the lower temperature dwell it is anticipated that (at least initially) polymerisation will result in linear polymer chains. In the meta substituted epoxy or amine, these chains will grow longer as they react earlier in the schedule. Later in the cure schedule, at higher temperatures, more crosslinking will occur and the final network structure achieved. In the para substituted epoxy or amine, the linear chains will be shorter resulting in a higher degree of crosslinking. Therefore, it is possible from this result to suggest that the meta substituted epoxy and amine have lower degrees of crosslinking in their networks than the para substituted equivalents. Correspondingly, the para substituted epoxy and amine show greater exothermic response between 265 and 280 °C (see Fig. 3). These high temperature reactions indicate a continuation of branching and crosslinking reactions and therefore the likelihood of a higher crosslink density.

3.2. Gas pycnometry

The average densities for the four sample types are given in Table 1 and illustrated in Fig. 4. (The individual density measurements for each sample type are provided in the data in brief article [37]). There is a clear increase in the density of the meta substituted TGMAP samples compared to the para substituted TGPAP equivalents. This suggests that when the phenylene ring is meta substituted the segments can pack more efficiently within the cured network due to an increase in conformational freedom. There may also be a contribution from the cure kinetics and the restriction of sub-T_g transition of the network. Cure kinetics, as mentioned previously, affect the network structure and it has been noted that packing density decreases with increased crosslinking [38]. This is due to the restriction of the network reducing the packing efficiency of chains which increases unoccupied volume. The restriction of phenylene ring rotational motions in the meta substituted networks results in a less intense beta transition and therefore less unoccupied volume. However, the latter is likely to have a small effect on the unoccupied volume.

When either isomer of TGAP is cured with the meta substituted DDS, the density increases slightly compared to the para substituted equivalent. This effect is less pronounced than that observed for the meta substituted TGMAP. This has been reported previously and was attributed to the meta substituted DDS having more conformational states available (cis and trans orientations) allowing for more efficient packing [39]. Again, contributions from the decreased crosslink density due to cure kinetics and the restriction of the beta transition in the meta substituted DDS may result in a reduction in unoccupied volume which causes an increased density. This result contradicts the established interpretation of differences observed in packing efficiencies between para and meta isomers which indicates that para isomers pack more effectively in the monomers.

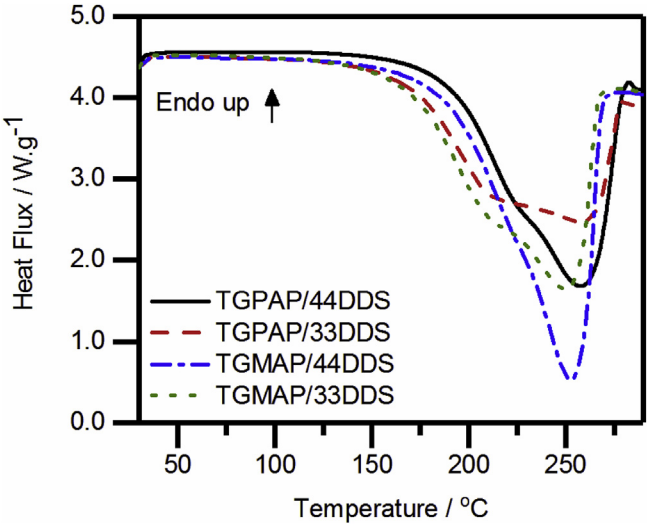

Fig. 3. Representative DSC curves of heat flux during cure against temperature for each of the four sample variants.

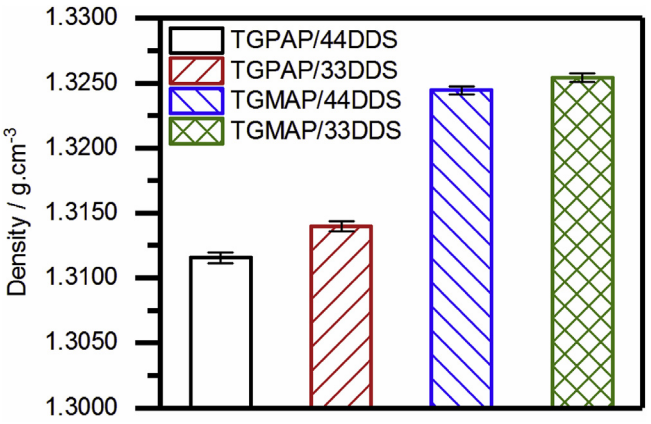

Fig. 4. Calculated density for the four sample variants. Graphical results correspond to an average of 3 samples. The error bars expressed in the graph is the standard deviation of the sample range.

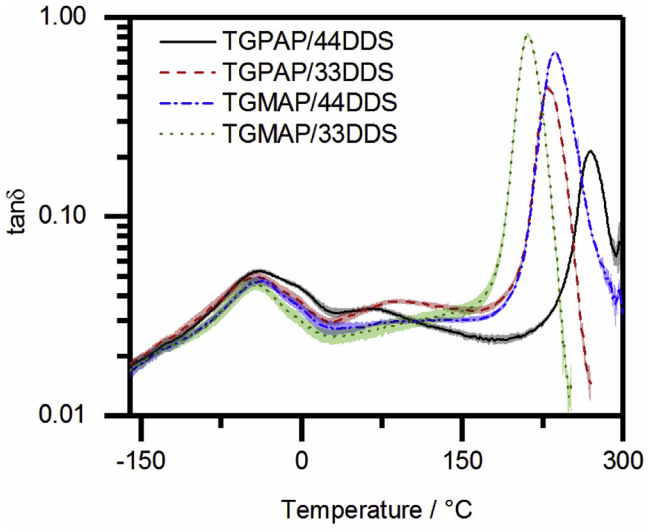

Fig. 5. Tanδ (logarithmic scale) against temperature for the four sample variants as measured by DMTA. Curves correspond to an average of 6 samples. The error bands expressed graphically are 95% confidence intervals.

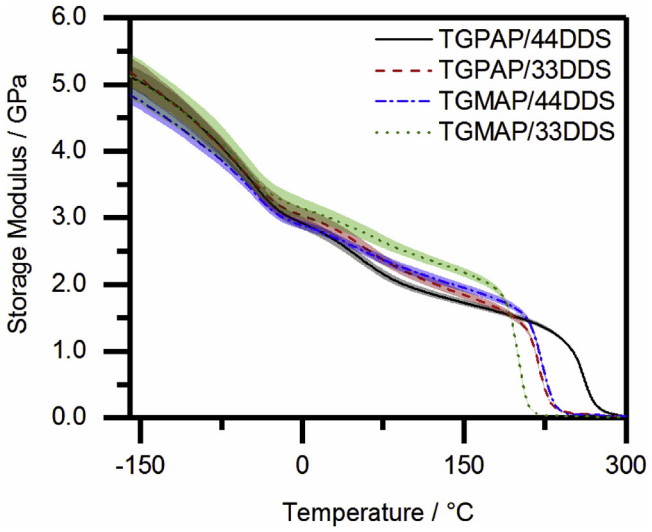

Fig. 6. Storage modulus against temperature for the four sample variants as measured by DMTA. Curves correspond to an average of 6 samples. The error bands expressed graphically are 95% confidence intervals.

3.3. Dynamic mechanical analysis

The average tanδ plots for the four samples types are provided in Fig. 5. (The individual dynamic mechanical analysis tanδ plots for each sample type are provided in the data in brief article [37]). Three secondary phase transitions are present between −160 °C and 300 °C at a frequency of 1 Hz for the four sample types. These consist of the beta transition centred around $T_\beta = -50$ °C, the omega transition centred around $T_\omega = 50$ °C and the glass transition over 200 °C.

3.3.1. Glass transition

The glass transition temperatures of each sample type are given in Table 1 and can be seen in the tanδ plots in Fig. 5. The T_g of the resins decreases on switching from the para substituted epoxy or amine to their meta equivalents. As a result, TGPAP/44DDS (para-para) has the highest T_g, TGMAP/33DDS (meta-meta) has the lowest T_g with TGMAP/44DDS (meta-para) and TGPAP/33DDS (para-meta) in between. The T_g is dependent on the mobility of the network and is therefore linked to the unoccupied volume, the cohesive energy and also the crosslink density. If T_g was solely controlled by the unoccupied volume, a higher T_g than observed would be expected for TGMAP/44DDS as the previously shown density results indicate better packing for this epoxy over the para equivalent. Correspondingly, a lower T_g for TGPAP/33DDS than observed would be expected as the lower density indicates poorer packing. However, the T_g's for both TGMAP/44DDS and TGPAP/33DDS are close to each other in value (237 and 231 °C respectively) confirming that the degree of crosslinking makes a significant and expected contribution to the T_g in these resins.

The T_g for TGMAP/44DDS is higher than in TGMAP/33DDS because there is more crosslinking in the former as suggested by the previously shown DSC results. Similarly, the T_g for TGPAP/33DDS is lower than TGPAP/44DDS because there is less crosslinking in the former. The reduced T_g in TGPAP/33DDS may also be related to the differences between the molecular motions that initiate the glass transition temperature.

The storage modulus plots for the four samples variants are shown in Fig. 6. Each of the secondary phase transitions is observable as a drop in the modulus at their characteristic temperatures. Comparison of the plots for the four samples variants reveals that below the glass transition, the meta substituted phenylene ring based networks are stiffer and above the glass transition, the opposite is true. This particular effect is often indicative of antiplasticisation.

3.3.2. Omega transition

The omega transition temperatures are given (where possible) in Table 1 and the peaks are shown graphically in Fig. 7. The omega transition is a small transition present in the temperature range 30–150 °C and is barely discernible in some sample types. The transition is far more pronounced in the para substituted TGPAP resins than the meta substituted TGMAP resins, irrespective of which isomer amine is used to cure the network. While the exact origin of the omega transition remains unclear, previous work has suggested it is caused by a larger segment of the network structure,

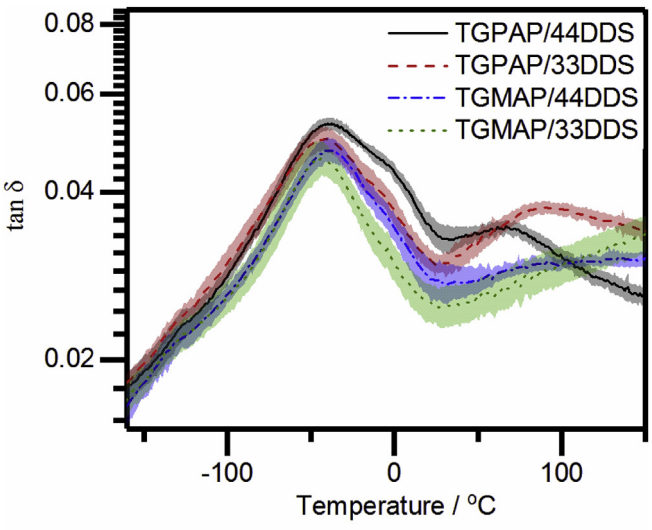

Fig. 7. DMTA trace of the beta transition and omega transition shown by tan delta (logarithmic scale) against temperature for the four sample variants. Curves correspond to an average of 6 samples. The error bands expressed graphically are 95% confidence intervals.

specifically the entire DGEBA segment in DGEBA/DDS [10]. This model can be used to interpret the trends seen in the four sample types used here. If the omega transition is caused by cooperative motion of a larger part of the network, then any restrictions in the motion of these segments will be observed as suppression of the omega peak. In Fig. 7, the omega transition is markedly less intense when the meta substituted TGAP is used compared to the para substituted equivalent because rotation of the phenylene rings in the former is restricted. This supports the hypothesis that the omega transition in TGAP based resins is caused by the combined cooperative motion of a segment consisting of the central phenylene ring and the hydroxypropyl ether groups.

Previous work has shown that the hydrogen bonded hydroxypropyl ether groups may contribute to the omega transition [25,26]. This could also be a contributing factor to the omega transition, which, although suppressed, has not disappeared in meta substituted epoxy resins. The omega transition peak temperature is higher in the meta substituted 33DDS networks which suggests a higher activation energy caused by a decreased unoccupied volume and higher cohesive energy within the network. The increased intensity of the omega transition in the meta substituted 33DDS networks also indicates more hydrogen bonded hydroxypropyl ether groups acting cooperatively with the phenylene ring.

3.3.3. Beta transition

The beta transition temperatures and tanδ peak areas are given in Table 1 and the peaks are shown graphically in Fig. 7. At −160 °C the loss tangent values for all four sample types are similar (at just less than 0.02) providing a convenient starting point for the analysis of the beta transition. As the temperature rises (on the cold side of the peak), the tanδ traces split into two pairs of lines where each line in the pair is approximately coincidental with the other. The higher tanδ pair corresponds to the para substituted TGPAP and the lower pair is the meta substituted TGMAP. The lower temperature region of the beta transition is associated with cooperative rotation of the phenylene rings in the epoxy parts of the network [10,24] as discussed previously. The beta transition intensity is reduced in the lower temperature region in the meta substituted TGMAP compared to the para substituted TGPAP because the rotation of the phenylene ring is restricted in the former. This is corroborated by observing that the amine used to cure the resin has no effect on the beta transition intensity in the lower temperature region. Using both the meta and para substituted amine makes no discernible difference to the beta transition intensity because the amine phenylene ring rotations are not activated until the temperature rises (see later).

As stated in the introduction, it should be noted that TGAP does not have the capacity to initiate cooperative motions of 'semi-adjacent' phenylene rings such as previously investigated [10]. In this work, the cold side of the beta transition has been linked to the phenylene ring rotations within the TGAP parts of the network. TGAP only contains a single phenylene ring indicating that the cold side of the beta transition is not solely caused by the rotation of phenylene rings separated by a C(Me)2 such as present in DGEBA.

As the temperature rises once more the beta transition reaches a maximum and the transition temperatures can be measured (see Table 1). The peak average value of T_β appears to be linked to the amine isomer as the value for both 33DDS cured resins is −43 °C and the values for the 44DDS cured resins are −37 and −39 °C. The middle temperature region of the beta transition is associated with the hydroxypropyl ether/amine groups in the network, which, as discussed earlier, should be approximately equal in number as the degrees of conversion are approximately equal. This is manifested in the beta transition temperatures which are of a similar magnitude irrespective of which amine isomer is present. However, the differences in the temperatures are relatively small and the transition is relatively broad so assigning meaningful conclusions to the beta transition temperatures is less rigorous than for the glass transition.

The heights of the peaks vary according to the sample type, following the same trend as seen in the higher temperature region of the beta transition (see later). However, a potentially more informative analysis of the peaks would be to measure the area under them, providing a measure of the total energy dissipated through the transition. Similar to the peak heights, the peak areas reported in Table 1 follow the same trend as seen in the higher temperature region of the beta transition. Unfortunately, the definition of the peak is obscured by not being able to clearly observe where they terminate. When the omega transition initiates, it overlaps with the end of the beta transition, this effect being more apparent in the para TGPAP samples than the meta equivalents.

Finally, as the temperature rises again (the hot side of the peak) the previously paired lines split into four distinct traces. The higher temperature region of the beta transition is associated with the cooperative rotation of the phenylene rings in the DDS parts of the network and now the influence of the DDS isomer is observed. Both meta substituted DDS samples have a lower beta transition intensity in this region than the para substituted equivalents. However, there is also a contribution from the epoxy in the higher temperature regions as the meta and para TGAP samples display a similar difference in beta transition intensity as seen in the low temperature regions. A reasonable explanation of this effect would be to suggest that the phenylene ring motions in the epoxy and amine parts of the network are coupled in some fashion and on the hot side of the beta transition peak, both effects are active to a greer or lesser extent.

3.4. Crosslink density

The calculated crosslink densities are given in Table 2 for the four sample types. Unfortunately, to obtain the rubbery modulus for TGPAP/44DDS a temperature of $T_g + 30 = 300\ ^\circ C$. is used where decomposition of this particular resin has started to occur. The onset of degradation in TGPAP/44DDS is also observed as an exothermic heat flow at the high temperature end of the DSC scan for this sample type, an effect which has been reported previously for TGPAP/44DDS [40]. Also, charring of the sample surface after it has been retrieved from the test machine is observed. Degradation of the resin will manifest as a lower than expected crosslink density as the high temperature severs covalent crosslinks. By contrast, the other three sample types used in this work are not subject to degradation at $T_g + 30$ so measuring the rubbery modulus and calculating the crosslink densities for these resins is valid.

As a result of network degradation, the crosslink density for TGPAP/44DDS is much lower than might be anticipated from the order of the glass transition temperatures reported earlier. The meta substituted TGMAP has a higher crosslink density when cured with the para substituted 44DDS and a lower crosslink density when cured with the meta substituted 33DDS. This result is in line with the DSC and glass transition temperature results shown earlier which suggest that the 33DDS cured resins have a lower crosslink density. A similar comparison can be made for TGPAP and TGMAP cured with 33DDS, where the former has a higher crosslink density than the latter, again agreeing with DSC and glass transition temperature results shown earlier. Combined together, the crosslink density results suggest that using either meta epoxy or meta amine results in a lower crosslink density compared to the para equivalents.

Table 2
Rubbery storage modulus, crosslink densities and compressive mechanical properties for the four sample types. The error expressed in the table is the standard deviation of the sample range.

Sample type	Rubbery Storage Modulus/MPa	Crosslink Density/mol.m^3	Young's Modulus/GPa	Strain to Failure/%	Yield Stress/MPa
TGPAP/44DDS	20.0 ± 4.6	1404 ± 320	3.31 ± 0.14	39.2 ± 2.8	–
TGPAP/33DDS	62.1 ± 4.0	4661 ± 299	3.68 ± 0.07	39.9 ± 1.5	189 ± 1
TGMAP/44DDS	43.0 ± 2.1	3186 ± 159	4.14 ± 0.14	47.8 ± 7.5	208 ± 1
TGMAP/33DDS	30.2 ± 6.8	2351 ± 54	4.48 ± 0.08	49.6 ± 13.2	214 ± 2

3.5. Compression testing

The results of static compression testing of the four sample types are shown in Fig. 8 and Table 2. (The individual stress-strain curves for each sample type are provided in the data in brief article [37]). The compressive modulus and yield stress values for the four sample types show a similar trend to that seen in the density measurements. The modulus and yield stress is highest when the packing efficiency of the molecules is highest as more material is present to support the applied load, i.e. when the density is highest. Higher moduli are observed when either a meta epoxy or meta amine is used instead of the para equivalents. These results agree with previous work which relates increases in the glassy modulus to decreases in unoccupied volume as the cohesive energy is increased [20,34,41].

Higher anelastic strain, as observed by an increased strain at yield has previously been attributed to the ability of the material to dissipate more energy due to local motions activated at the beta transition [33]. Here, the para substituted phenylene ring variants show a higher yield strain and therefore a higher anelastic strain is anticipated in these. Correspondingly, the intensity of the beta transition is increased in the para substituted phenylene ring networks which agrees with the previously reported work.

The extent of strain softening post yield varies among the sample types. In TGMAP/33DDS there is a clear yield point followed by marked post yield strain softening. The extent of strain softening reduces as more para substituted phenylene rings are used until TGPAP/44DDS where there is no strain softening at all. In this particular sample type, the definition of yield point used in the analysis fails. Strain softening is caused by post yield plastic flow which has previously been related to large scale reorientation in DDS cured epoxy networks [33]. The hypothesis put forward to explain differences in the meta and para substituted networks is that a segment rotation may occur in 33DDS which is not present in 44DDS linear chains [33]. Correspondingly, in the meta substituted TGMAP networks an increase in strain softening is observed and it is suggested that segment rotation may also occur, most likely a rotation of either of the phenylene ring bonds. Post yield, there are fewer intermolecular interactions holding the polymer chains together facilitating these larger scale reorientations. The lower crosslink density seen in the meta substituted epoxy or amine containing resins indicates there is less restriction on large scale reorientation of the network under compressive loads. In the para equivalents, the crosslink density was higher to begin with, to the extent that the para-para TGPAP/44DDS has a lower capacity to soften and doesn't display a yield point (under the definition used).

The increased reorientation of chains as well as reduced crosslink density within the meta substituted sample types leads to an increase in the strain to failure values. The higher densities of the meta substituted sample types indicates more material is supporting the applied load and therefore higher strains are needed to cause failure. This is supported by the increased crosslink density of the para substituted sample types shown earlier in the DSC and T_g analyses. Both an increased crosslink density and T_g suggests that the para substituted samples types are more brittle than the meta substituted equivalents as the crosslinking restricts plastic flow of the network.

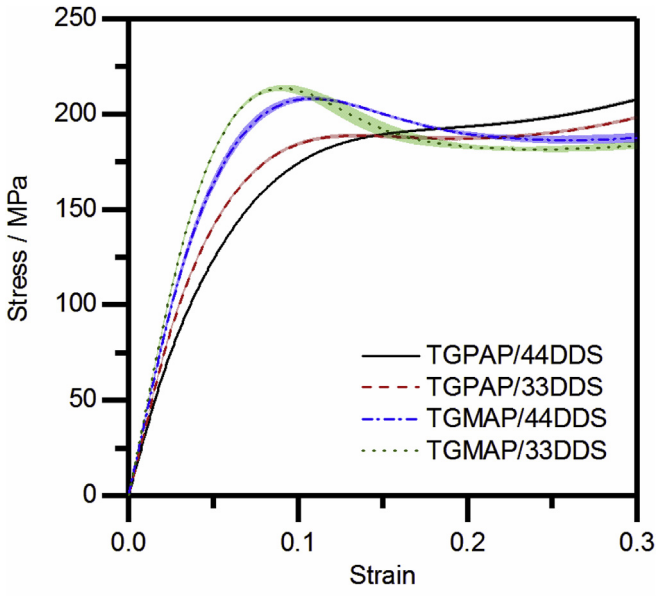

Fig. 8. Compressive stress-strain curves for the four sample variants. Curves correspond to an average of 5 samples. The error bands expressed graphically are 95% confidence intervals.

3.6. Single Edge Notched Beam testing

SENB testing was performed for each sample type and the calculated critical stress intensities and critical energy release rates are given in Table 3 with the former being illustrated in Fig. 9. The results show that the toughness of the network is increased when the meta substituted 33DDS is used over the para substituted 44DDS. Conversely, the toughness shows very little change when the meta substituted TGMAP is used over the para substituted TGPAP. Although the origin of this effect is not clear, the fracture toughness is not solely related to cohesive properties within the network as it also relies on the plastic behaviour of the material [42]. Therefore fracture toughness is related to both the chemical and network structure [42] and does not simply depend on the crosslink density [43].

Table 3
Calculated critical stress intensities and critical energy release rates from single edge notched beam testing for the four sample variants. Values are averages of at least 17 tests. The error expressed in the table is the standard deviation of the sample range.

Sample type	K_{IC}/MPa.m$^{1/2}$	G_{IC}/kJ.m^{-2}
TGPAP/44DDS	0.61 ± 0.05	0.12 ± 0.04
TGPAP/33DDS	0.68 ± 0.06	0.14 ± 0.04
TGMAP/44DDS	0.59 ± 0.06	0.11 ± 0.04
TGMAP/33DDS	0.66 ± 0.07	0.13 ± 0.07

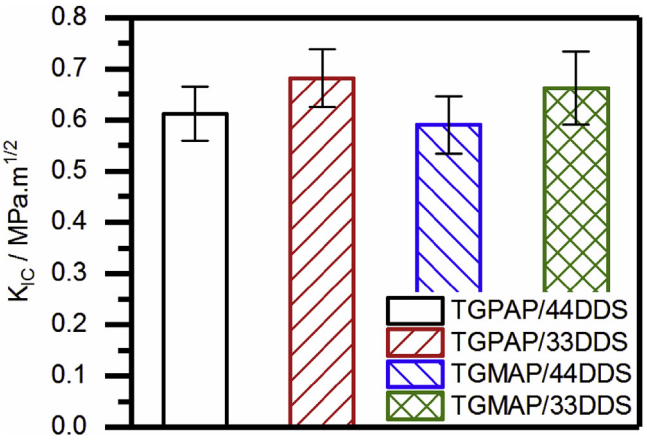

Fig. 9. Calculated critical stress intensity (K_{IC}) results for the four sample types. Graphical results correspond to at least 17 samples. The error bars expressed in the graph is the standard deviation of the sample range.

The differences in the chemical structure of the four variants is due to the substitution position on the phenylene rings. As mentioned previously, the meta substituted 33DDS can adopt a cis or trans conformation which is not possible in the para substituted 44DDS. This suggests the fracture toughness increases observed in the 33DDS cured resins are caused by the conformational freedom associated with its phenylene rings. Despite results presented earlier suggesting conformational freedom is a significant factor in the density and strain softening in the meta substituted TGMAP, the fracture toughness values are independent of the phenylene ring substitution in the epoxy.

The network structure of the resins is another factor in the observed differences in the fracture toughness. The effect of switching isomer can be interpreted in terms of the packing efficiency, intermolecular interactions and crosslink density of the network. The density of the meta substituted resin is higher than the para substituted equivalents suggesting packing efficiency and the chance of intermolecular interactions is higher. The DSC analysis and rubbery modulus suggest a lower crosslink density in the meta substituted resin compared to the para substituted equivalents. However, this effect is not exclusive to the amine structure and will also have contributions from the epoxy parts of the network. It is therefore a complicated contribution of these effects that dictates the fracture toughness properties.

4. Conclusions

The results presented in this work strongly indicate that replacing the para substituted phenylene rings in the network with meta substituted phenylene rings results in antiplasticisation. In this case, internal antiplasticisation is occurring, the requirements for which can vary slightly from case to case but in general they can be stated as follows. Internal antiplasticisation causes an increase in glassy modulus, yield stress, density, strain to failure and fracture toughness, though the latter exhibits inconsistent behaviour. Also, it causes a reduction in glass transition temperature, the intensity of the beta transition and the rubbery modulus. Results presented here for the four epoxy variants show an increase in glassy modulus (see Fig. 8 and Table 2), yield stress (see Fig. 8 and Table 2), density (see Fig. 4 and Table 1), strain to failure (see Table 2) and the fracture toughness (see Fig. 9 and Table 3) for the meta substituted phenylene ring networks. Correspondingly, decreases are seen in the glass transition temperature (see Fig. 5 and Table 1), intensity of the beta transition (see Fig. 7 and Table 1) and the rubbery modulus (see Fig. 6 and Table 2) for the meta substituted phenylene ring networks.

A primary difference noted between antiplasticisation caused by the addition of fillers and internal antiplasticisation is the strain to failure. Within antiplasticised networks by the addition of fillers, the antiplasticisers occupy the unoccupied volume and increase the restriction to plastic flow within the network. Conversely, internal antiplasticisation observed in this study by structural isomeric changes shows distinct variations in the network structure. The decreased crosslink density within meta substituted networks allows for plastic flow within these antiplasticised networks causing increased strain to failure.

The effects on glassy modulus, yield stress, density, glass transition temperature and the intensity of the beta transition as a result of internal antiplasticisation are rationalized in terms of improvements in packing efficiency and cohesive energy due to the meta substitution. Changes in the rubbery modulus and to some extent the glass transition temperature are described in terms of the cure kinetics. Here, the more reactive meta substituted epoxies or amines result in a more linear, less crosslinked network compared to the para substituted equivalents. The fracture toughness results don't entirely fit with either of these interpretations but can be linked to the increased conformational freedom in the meta substituted phenylene ring amines.

Conflicts of interest

None.

Funding sources

This work was supported by the UK Engineering and Physical Sciences Research Council (EP/M508135/1).

Acknowledgments

The authors gratefully acknowledge Huntsman Advanced Materials for supplying TGPAP (Araldite MY0510) and TGMAP (Araldite MY0610) epoxy resins and 33DDS (Aradur 9719-1) hardener used in this study.

Appendix A. Supplementary data

Supplementary data related to this article can be found at https://doi.org/10.1016/j.polymer.2018.05.048.

References

[1] R.J. Varley, J.H. Hodgkin, D.G. Hawthorne, G.P. Simon, Toughening of a trifunctional epoxy system.II. Thermal characterization of epoxy/amine cure, J. Appl. Polym. Sci. 60 (12) (1996) 2251–2263.
[2] Epoxy Resins Chemistry and Technology, second ed., Marcel Dekker, Inc, New York, 1988.
[3] R.J. Varley, J.H. Hodgkin, G.P. Simon, Toughening of a trifunctional epoxy system - Part VI. Structure property relationships of the thermoplastic toughened system, Polymer 42 (8) (2001) 3847–3858.
[4] D.J. Hourston, J.M. Lane, The toughening of epoxy resins with thermoplastics: 1. Trifunctional epoxy resin-polyetherimide blends, Polymer 33 (7) (1992) 1379–1383.
[5] X.L. Cheng, Q. Wu, S.E. Morgan, J.S. Wiggins, Morphologies and mechanical properties of polyethersulfone modified epoxy blends through multifunctional epoxy composition, J. Appl. Polym. Sci. 134 (18) (2017) 44775–44785.
[6] D. Ratna, G.P. Simon, Thermal and mechanical properties of a hydroxyl-functional dendritic hyperbranched polymer and trifunctional epoxy resin blends, Polym. Eng. Sci. 41 (10) (2001) 1815–1822.
[7] D. Ratna, R. Varley, G.P. Simon, Toughening of trifunctional epoxy using an epoxy-functionalized hyperbranched polymer, J. Appl. Polym. Sci. 89 (9) (2003) 2339–2345.
[8] I. Blanco, G. Cicala, C. Lo Faro, O. Motta, G. Recca, Thermomechanical and morphological properties of epoxy resins modified with functionalized

hyperbranched polyester, Polym. Eng. Sci. 46 (11) (2006) 1502–1511.
[9] G. Cicala, A. Recca, C. Restuccia, Influence of hydroxyl functionalized hyperbranched polymers on the thermomechanical and morphological properties of epoxy resins, Polym. Eng. Sci. 45 (2) (2005) 225–237.
[10] J.W. Tu, S.J. Tucker, S. Christensen, A.R. Sayed, W.L. Jarrett, J.S. Wiggins, Phenylene ring motions in isomeric glassy epoxy networks and their contributions to thermal and mechanical properties, Macromolecules 48 (6) (2015) 1748–1758.
[11] S. Pandini, F. Bignotti, F. Baldi, L. Sartore, G. Consolati, G. Panzarasa, Thermomechanical and large deformation behaviors of antiplasticized epoxy resins: effect of material formulation and network architecture, Polym. Eng. Sci. 57 (6) (2017) 553–565.
[12] J. Daly, A. Britten, A. Garton, P.D. McLean, An additive for increasing the strength and modulus of amine-cured epoxy resins, J. Appl. Polym. Sci. 29 (4) (1984) 1403–1414.
[13] N. Hata, R. Yamauchi, Viscoelastic properties of epoxy resins.II. Antiplasticization in highly crosslinked epoxy system, J. Appl. Polym. Sci. 17 (7) (1973) 2173–2181.
[14] W.J. Jackson, J.R. Caldwell, Antiplasticization.II. Characteristics of antiplasticizers, J. Appl. Polym. Sci. 11 (2) (1967) 211–226.
[15] J.-P. Pascault, H. Sautereau, J. Verdu, R.J.J. Williams, Thermosetting Polymers, Marcel Dekker Inc, New York, 2002.
[16] Y.G. Won, J. Galy, J.F. Gerard, J.P. Pascault, V. Bellenger, J. Verdu, Internal antiplasticization in copolymer and terpolymer networks based on diepoxides, diamines and monoamines, Polymer 31 (9) (1990) 1787–1792.
[17] L. Heux, F. Laupretre, J.L. Halary, L. Monnerie, Dynamic mechanical and C-13 nmr analyses of the effects of antiplasticization on the beta secondary relaxation of aryl-aliphatic epoxy resins, Polymer 39 (6–7) (1998) 1269–1278.
[18] N. Hata, J. Kumanotani, Viscoelastic properties of epoxy resins. III. Effect of molecular weight of antiplasticizers in highly crosslinked antiplasticization system, J. Appl. Polym. Sci. 21 (5) (1977) 1257–1266.
[19] P.D. McLean, R.F. Scott, A. Garton, Fortifiers for epoxy-amine systems, Br. Polym. J. 15 (1) (1983) 66–70.
[20] E. Morel, V. Bellenger, M. Bocquet, J. Verdu, Structure-properties relationships for densely cross-linked epoxide amine systems based on epoxide or amine mixtures .3. Elastic properties, J. Mater. Sci. 24 (1) (1989) 69–75.
[21] G.R. Palmese, R.L. McCullough, Effect of epoxy amine stoichiometry on cured resin material properties, J. Appl. Polym. Sci. 46 (10) (1992) 1863–1873.
[22] J. Boye, P. Demont, C. Lacabanne, Secondary retardation modes in diglycidyl ether of bisphenol A-diamino diphenyl methane networks, J. Polym. Sci. B Polym. Phys. 32 (8) (1994) 1359–1369.
[23] A.C. Grillet, J. Galy, J.F. Gerard, J.P. Pascault, Mechanical and viscoelastic properties of epoxy networks cured with aromatic diamines, Polymer 32 (10) (1991) 1885–1891.
[24] J.F. Shi, P.T. Inglefield, A.A. Jones, M.D. Meadows, Sub-glass transition motions in linear and cross-linked bisphenol-type epoxy resins by deuterium line shape NMR, Macromolecules 29 (2) (1996) 605–609.
[25] M. Ochi, M. Shimbo, M. Saga, N. Takashima, Mechanical and dielectric relaxations of epoxide resins containing spiro-ring structure, J. Polym. Sci. B Polym. Phys. 24 (10) (1986) 2185–2195.
[26] M. Ochi, T. Shiba, H. Takeuchi, M. Yoshizumi, M. Shimbo, Effect of the introduction of methoxy branches on low-temperature relaxations and fracture toughness of epoxide resins, Polymer 30 (6) (1989) 1079–1084.
[27] V.B. Gupta, L.T. Drzal, C.Y.C. Lee, M.J. Rich, The effects of stoichiometry and structure on the dynamic torsional properties of a cured epoxy resin system, J. Macromol. Sci., Phys. B23 (4–6) (1985) 435–466.
[28] J.D. Keenan, J.C. Seferis, J.T. Quinlivan, Effects of moisture and stoichiometry on the dynamic mechanical properties of a high-performance structural epoxy, J. Appl. Polym. Sci. 24 (12) (1979) 2375–2387.
[29] O. Delatyck, J.C. Shaw, J.G. Williams, Viscoelastic properties of epoxy-diamine networks, J. Polym. Sci. 2 Polym. Phys. 7 (5PA2) (1969) 753–762.
[30] I. Harismendy, R. Miner, A. Valea, R. LlanoPonte, F. Mujika, I. Mondragon, Strain rate and temperature effects on the mechanical behaviour of epoxy mixtures with different crosslink densities, Polymer 38 (22) (1997) 5573–5577.
[31] S.R. Heinz, Development and Utilization of Digital Image Correlation Techniques for the Study of Structural Isomerism Effects on Strain Development in Epoxy Network Glasses, Graduate School, The University of Southern Mississippi, 2011.
[32] R.J. Varley, G.R. Heath, D.G. Hawthorne, J.H. Hodgkin, G.P. Simon, Toughening of a trifunctional epoxy system .1. Near-infrared spectroscopy study of homopolymer cure, Polymer 36 (7) (1995) 1347–1355.
[33] S. Heinz, J.W. Tu, M. Jackson, J. Wiggins, Digital image correlation analysis of strain recovery in glassy polymer network isomers, Polymer 82 (2016) 87–92.
[34] A.J. Lesser, E. Crawford, The role of network architecture on the glass transition temperature of epoxy resins, J. Appl. Polym. Sci. 66 (2) (1997) 387–395.
[35] L. Bonnaud, J.P. Pascault, H. Sautereau, Kinetic of a thermoplastic-modified epoxy-aromatic diamine formulation: modeling and influence of a trifunctional epoxy prepolymer, Eur. Polym. J. 36 (7) (2000) 1313–1321.
[36] R.D. Patel, R.G. Patel, V.S. Patel, Investigation of kinetics of curing of triglycidyl-p-aminophenol with aromatic diamines by differential scanning calorimetry, J. Therm. Anal. Calorim. 34 (5–6) (1988) 1283–1293.
[37] R. Ramsdale-Capper, J.P. Foreman, Data from static and dynamic mechanical tests of different isomers of amine cured multifunctional epoxy resins, Data in Brief.
[38] V. Bellenger, W. Dhaoui, E. Morel, J. Verdu, Packing density of the amine-crosslinked stoichiometric epoxy networks, J. Appl. Polym. Sci. 35 (3) (1988) 563–571.
[39] M. Jackson, M. Kaushik, S. Nazarenko, S. Ward, R. Maskell, J. Wiggins, Effect of free volume hole-size on fluid ingress of glassy epoxy networks, Polymer 52 (20) (2011) 4528–4535.
[40] J.M. Hutchinson, F. Shiravand, Y. Calventus, I. Fraga, Isothermal and non-isothermal cure of a tri-functional epoxy resin (TGAP): a stochastic TMDSC study, Thermochim. Acta 529 (2012) 14–21.
[41] N. Hata, J. Kumanota, Viscoelastic properties of epoxy resin.I. Effect of prepolymer structure on viscoelastic properties, J. Appl. Polym. Sci. 15 (10) (1971) 2371–2380.
[42] V.B. Gupta, L.T. Drzal, C.Y.C. Lee, M.J. Rich, The temperature-dependence of some mechanical properties of a cured epoxy resin system, Polym. Eng. Sci. 25 (13) (1985) 812–823.
[43] R. Rahul, R. Kitey, Effect of cross-linking on dynamic mechanical and fracture behavior of epoxy variants, Compos. B Eng. 85 (2016) 336–342.